Integrated Metagenomic and Metabolomic Analyses of the Effects of Total Flavonoids of Rhizoma Drynariae on Reducing Ovariectomized-Induced Osteoporosis by Regulating Gut Microbiota and Related Metabolites

Qiuyue Li
Wangjing Hospital of China Academy of Chinese Medical Sciences
Shengjie Fang
Wangjing Hospital of China Academy of Chinese Medical Sciences
Xuelei Chu
Wangjing Hospital of China Academy of Chinese Medical Sciences
Jia Zhu
Wangjing Hospital of China Academy of Chinese Medical Sciences
Qinghui Song
Wangjing Hospital of China Academy of Chinese Medical Sciences
Xu Wei
Wangjing Hospital of China Academy of Chinese Medical Sciences
Chaolu Wang
Wangjing Hospital of China Academy of Chinese Medical Sciences
Chengzhi Hou (houcz2010@163.com)
Wangjing Hospital of China Academy of Chinese Medical Sciences

Article

Keywords: osteoporosis, total flavonoids of rhizoma drynariae, metagenomics, metabolomics, Akkermansia muciniphila

Posted Date: October 25th, 2022

DOI: https://doi.org/10.21203/rs.3.rs-2147791/v1

Abstract

Ethnopharmacological relevance:

Total flavonoids of Rhizoma Drynariae (TFRD), an important component extracted from the dried rhizome of *Drynaria roosii* Nakaike [Polypodiaceae]. TFRD has been widely used in China to treat osteoporosis (OP). However, the specific molecular mechanism of TFRD against OP has not been fully clarified.

Aim of the study:

The aim of this study was to further elucidate molecular mechanism of TFRD for treating OP based on metagenomic and metabolomic analyses.

Materials and methods:

In this study, hematoxylin-eosin (H&E) staining, micro computed tomography (micro-CT) and bone mineral density (BMD) analysis were used to observe pharmacological effects of TFRD against ovariectomized (OVX)-induced OP. Subsequently, multiomics analysis including metagenomics, untargeted and short chain fatty acids (SCFAs) metabolomics were carried out to identify whether the anti-osteoporosis mechanism of TFRD correlated with gut microbiota and related metabolites.

Results:

TFRD could improve the microstructure and density of trabecular bone in OVX rats. 17 differential species, which mainly from *Akkermansia, Bacteroides,* and *Phascolarctobacterium*genus, 14 related differential metabolites and acetic acid in SCFAs were significantly altered by OVX and reversed by TFRD. Furthermore, according to results of untargeted metabolomics analysis, it was found several metabolic pathways such as phenylalanine metabolism, phenylalanine, tyrosine and tryptophan biosynthesis and so on might play an important role in TFRD against OP. In order to further study the relationship between gut microbiota and related metabolites, spearman correlation analysis was used, and showed that gut microbiota such as *Akkermansia muciniphila* might be closely related to several metabolites and metabolic pathways.

Conclusions:

TFRD treatment could reduce the effects of OVX-induced OP by altering community composition and abundance of gut microbiota, regulating metabolites and SCFAs. It was speculated that the gut microbiota especially *Akkermansia muciniphila* and related metabolites might play an important role in TFRD against OP, and deserve further study by follow-up experiment. This conclusion provides new theoretical support for mechanism research of TFRD against OP.

Highlights

For the first time, TFRD could improve OVX-induced OP by increasing abundance of *Akk.*

TFRD could reduce the effects of OVX-induced OP by HE, microCT and BMD analysis.

We used metagenomics, untargeted and SCFAs to investigate the specific mechanism.

1. Introduction

Postmenopausal osteoporosis (PMOP) is a type of skeletal disease caused by estrogen deficiency and characterized by osteopenia and bone microarchitecture destruction, which can induce an increased incidence of fragility fractures[1]. PMOP has problems such as high incidence, hidden disease, many complications, complex mechanism, limited drug treatment and so on. It is of great theoretical value and clinical application prospect to explore new pathogenesis of OP and innovative therapy. Since Swedish scientists first discovered that gut microbiota can increase bone mineral density in mice in 2012, the relationship between gut microbiota and OP has become a hot spot in orthopaedic research in recent years[2]. In 2020, Chevalier et al. researched that warmth can prevent OP by regulating gut microbiota[3]. He et al. compared the characteristics of gut microbiota and metabolites in 106 postmenopausal women and found that the abundance and diversity of gut microbiota in OP patients and healthy people were significantly different[4]. Qin et al. conducted a metagenome analysis of gut microbiota in 88 subjects from the First Affiliated Hospital of Zhengzhou University from 2018 to 2019 (28 patients with OP and 60 controls)[5]. Some species decreased (such as *Streptococcus*, etc.), while some species increased (such as *Bacteroides*, etc.). Therefore, it is of great clinical significance to find drugs treating OP through gut microbiota and to dig into its action mechanism. The study of gut microbiota to improve OP can provide new ideas and strategies for the treatment of OP.

The “gut microbiota-bone” axis is based on the interconnection between the bone and the gut [6]. The gut microbiota can produce a variety of molecules such as enzymes, short-chain fatty acids (SCFAs), and metabolites. Lipopolysaccharide (LPS), the main component of the cell wall of gram-negative bacteria, increases in conditional pathogenic bacteria, continuously produces LPS into the blood circulation, induces an inflammatory response in the body, and reduces a large number of bifidobacterial with the function of protecting the intestinal barrier, making the intestinal the permeability of the tract mucosa increased.

Modern medical research has shown that the imbalance of gut microbiota can lead to abnormal immune regulation, up-regulation of inflammatory factor expression, and promotion of osteoclast differentiation, thereby aggravating bone resorption and inducing the occurrence of OP[7]. In 2021, Liu et al. published research results in the top international journal "Advanced Science", proving that *Akkermansia muciniphila* promotes bone formation and inhibition in castrated mice [8]. In summary, the gut microbiota can be deeply explored as a potential target for the treatment of OP[9]. However, the mechanism by which the gut microbiota regulates OP is still under study. In the future, the composition of gut microbiota may

be able to predict the risk of OP and fractures, and the regulation of the gut microbiota may become a new target for the treatment of OP.

Nowadays, traditional Chinese medicine (TCM) and its components have become a good choice for the prevention and treatment of OP with their positive curative effect and small side effects in clinic, and have been widely accepted[10,11]. Total flavonoids of Rhizoma Drynariae (TFRD) is an important component extracted from the dried rhizome of *Drynaria roosii* Nakaike [Polypodiaceae]. *Drynaria roosii* Nakaike, a perennial pteridophyte, was first recorded in < BEN CAO SHI YI > of the Tang Dynasty more than 1000 years ago, and have the function with tonifying kidney and bone [12](Zhang et al., 2022). TFRD have definite clinical effect in the treatment of OP, and the curative effect in the treatment of ovariectomized (OVX)-induced OP in rats is remarkable. In recent years, TFRD have been widely used in orthopaedical diseases in Asian countries with pharmacological effects of promoting osteogenesis, anti-inflammatory and antioxidant [13,14]. Meta-analysis showed that TFRD alone or in combination could significantly improve bone mineral density, and play an important role in the prevention of OP[15]. Furthermore, several studies found that TFRD could protect bone health, promote osteoblast differentiation and maturation, and inhibit osteoclast formation. Shen et al. revealed mechanism of TFRD against OP by osteoclast-related pathway promoting H-type angiogenesis and Song et al. told us TFRD inhibited osteoclastogenesis via up-regulating osteoprotegrin, as well as down-regulating receptor activator of nuclear factor kappa-B ligand (RANKL) expression[16,17].

It was well known that the bioavailability of flavonoids is very low, flavonoids can be widely metabolized by gut microbiota and gut microbiota plays a key role in the pharmacological activity of flavonoids. Moreover, flavonoids can directly or indirectly regulate the relative abundance and activity of gut microbiota and change the physiological state of intestinal microenvironment [18,19]. Therefore, it is speculated that the regulation of gut microbiota and related metabolites might play an important role in the TFRD against OP. This study intends to further clarify its pharmacodynamic mechanism from the perspective of mechanism of action. We selected OVX rats as OP model and investigated the therapeutic effect of TFRD [20,21]. Subsequently, we used metagenomics, untargeted and SCFAs metabolomics analysis to investigate the specific mechanism of TFRD against OP by hematoxylin-eosin (H&E), micro computed tomography (micro-CT) and bone mineral density (BMD) analysis, and to identify whether anti-osteoporosis mechanism of TFRD correlated with regulation of gut microbiota and related metabolites, so as to provide new theoretical support for mechanism research of TFRD against OP.

2. Materials And Methods

Ethics statement

In this study, all methods were performed in accordance with relevant guidelines and regulations, and the reporting in the manuscript follows the recommendations in the ARRIVE guidelines. All animal care and experimental protocols and procedures had been approved by the Laboratory Animal Center Institute of

Basic Theory for Chinese Medicine, China Academy of Chinese Medicine Science. Animal certificate number: 110324201102334251.

2.1. Reagents and materials

TFRD (Batch number: 200706) was purchased from Beijing Qihuang Pharmaceutical Co., Ltd (Beijing, China). Alendronate (ALN) enteric-coated tablets (Batch number: 266210501) was purchased from CSPC Ouyi Pharmaceutical Co., Ltd (Shijiazhuang, China). Ethylenediaminetetraacetic acid (EDTA) was purchased from Solarbio (PRC). Hematoxylin-eosin (H&E) was purchased from Baso (PRC).

In our previous work, the dose of TFRD against OP and the chemical composition of TFRD have been analyzed and identified [22](Zhang et al., 2022). The equivalent dose for rats was obtained using the formula as follows: Animal equivalent dose (mg/kg) = Human dose (mg/kg) * Human Km/Animal Km. The constituents of TFRD was obtained by ultra-high-performance liquid chromatography coupled with electrospray ionization quadrupole time-of-flight mass spectrometry (UHPLC-ESI-Q-TOF-MS) analysis. A total of 191 constituents including naringin, naringenin, kaempferitrin, kaempferol, luteolin, eriodictyol, cianidanol, etc., were then identified[22] (Zhang et al., 2022).

2.2. Animal Study

60 Sprague-Dawley rats (8 weeks old, 220 ± 10g) were purchased from SPF Biotechnology Co., Ltd (Beijing, PRC). All rats were raised in a standard laboratory condition (temperature: 22 ± 1℃, humidity: 50 ± 10%, 12:12 h light/dark cycle, free specific pathogen), feeding with free drinking water and food. The detailed protocol was approved by the institutional Animal Ethics Committee. After 7-day circumstances adaptation, all rats were randomly divided into sham 1 group, model 1 group, sham 2 group, model 2 group, TFRD group, ALN group (n = 10 per group). Then all rats in the model, TFRD, ALN group underwent bilaterally ovariectomy after anesthesia. For sham group, only the adipose tissue on one side of the ovary was removed and other operations were the same as the surgery groups. All rats were fed normally for 12 weeks after operation. This study was approved by the Ethics Committee of Chinese Academy of Chinese Medical Sciences with the ethics approval number of IBTCMCACMS21-2108-01.

After 12 weeks of bilateral ovariectomy, the rats in sham 1 and model 1 group were euthanatized, and then tibia and femur of them were collected for histology, micro-CT and BMD analysis to determine whether OVX rat model was established successfully. Meanwhile, the rats in other four groups were given a 12-week intervention. The rats in TFRD group and ALN group were orally administered with TFRD (67.5 mg/kg/d) and ALN (1 mg/kg/d), respectively. The rats in sham 2 and model 2 group were given the equivalent volume of normal saline. At the end of the experiment, pentobarbital (40 mg/kg) was injected intraperitoneally according to the weight. The tibia, femur, feces and serum of all rats were collected for subsequent histology, micro-CT, BMD, metagenomic, untargeted and SCFAs metabolomic analysis.

2.3. Histology analysis

The left tibia of rats was fixed with 4% formaldehyde, and then decalcified with 10% EDTA. Subsequently, the samples were embedded in paraffin and sectioned at a thickness of 5-μm. At last, the sections were stained with H&E and photographed with a microscope (Olympus, Japan).

2.4. Micro computed tomography analysis

The right femur of rats was fixed with 4% formaldehyde, and decalcified with 10% EDTA. Subsequently, the femur was scanned by Skyscan 1276 micro-CT (Bruker, USA). The lowest end of the distal femoral growth plate was set as the analysis reference line, and the area with a thickness of 3mm was set as the region of interest (ROI). The 3D image was reconstructed with NRecon software and analyzed with DataViewer, CTvox and CTan software.

2.5. Bone mineral density analysis

The right tibia of rats was collected for BMD analysis. BMD of rats were detected by Dual energy X-ray absorptiometry and analyzed by Osteocore 3 BMD analysis software.

2.6. Metagenomics analysis

The microbial genomic DNA was extracted from feces of rats using DNeasy PowerWater Kit (MoBio/QIAGEN, USA) and detected by Quantifluor-ST fluorometer (Promega, USA) and Quant-iT PicoGreen dsDNA Assay Kit (Invitrogen, USA). Then the qualified DNA samples were randomly fragmented to a size with 350 bp by Covaris ultrasonic crusher (Covaris, USA). The DNA library was constructed by end repair, adding A tail, ligating sequencing primer, purification and PCR amplification. The insert size of the library was assessed by Agilent 2100 (Agilent Technologies, Germany), and the effective concentration of the library was accurately quantified by Q-PCR (the effective concentration of the Library > 3nM). Then the DNA library were sequenced on Illumina NovaSeq/HiSeq (Illumina, USA) to obtain raw data according to the manufacturer's instructions. Subsequently, clean reads was obtained by filtering out low-quality. After single and hybrid assembly, a non-redundant gene catalogue was constructed by clustering. Then non-redundant gene catalogue was predicted using MetaGeneMark, and aligned to NCBI NR library for further species annotation. Based on the gene abundance table, species abundances profile at different taxonomic levels were obtained.

2.7. Untargeted Metabolomics analysis

Serum samples of rats were used for untargeted metabolomics. 100 μL of each sample was transferred into 2 mL centrifuge tubes, added 400 μL of methanol, vortexed and centrifuged to obtain all supernatant and then dried in vacuum. Dissolved samples with 150 μL 2-chlorobenzalanine (4 ppm) 80% methanol solution, and filtered the supernatant through 0.22 μm membrane to obtain the prepared samples. The quality control samples consisted of 20 μ L in each prepared sample for Liquid Chromatography-Mass Spectrometry (LC-MS) detection.

Chromatographic separation was accomplished in a Thermo Ultimate 3000 system (Thermo Scientific, USA) equipped with an ACQUITY UPLC® HSS T3 (150×2.1 mm, 1.8 μm, Waters) column maintained at 40

℃. 2 μL of each sample performed for gradient elution was carried out with 0.1% formic acid in water (C) and 0.1% formic acid in acetonitrile (D) or 5 mM ammonium formate in water (A) and acetonitrile (B) at a flow rate of 0.25 mL/min. The linear gradient elution setting was as follows: 0 ~ 1 min, 2% B/D; 1 ~ 9 min, 2%~50% B/D; 9 ~ 12 min, 50%~98% B/D; 12 ~ 13.5 min, 98% B/D; 13.5 ~ 14 min, 98%~2% B/D; 14 ~ 20 min, 2% D-positive model (14 ~ 17 min, 2% B-negative model). After chromatographic separation, the Electrospray ionization source experiments were executed on the Thermo Q Exactive Plus mass spectrometer (Thermo Scientific, USA). The setting was as follows: the spray voltage was 3.5 kV and −2.5 kV in positive and negative modes respectively, sheath gas and auxiliary gas were 30 and 10 arbitrary units respectively, capillary temperature was 325 ℃. The analyzer scanned over a mass range of m/z 81 − 1 000 for full scan at a mass resolution of 70 000. Data dependent acquisition MS/MS experiments were performed with HCD scan. Dynamic exclusion was implemented to remove some unnecessary information in MS/MS spectra.

2.8. SCFAs metabolomics analysis

Feces samples of rats were used for metabolomics of SCFAs. Samples were supplemented with 15% phosphoric acid, internal standard (isohexanoic acid) solution and ether, homogenized for 1 min. The supernatant was detected for gas chromatography-mass spectrometer analysis by Thermo TRACE 1310 gas chromatograph system (Thermo Scientific, USA) coupled with a Thermo ISQ LT mass spectrometer (Thermo Scientific, USA). Helium was used as the carrier gas with a flow rate at 1.0 ml/min in an Agilent HP-INNOWAX capillary column (30 m×250 μm×0.25 μm). 1 μL of the analyte was injected in split mode (10:1).

2.9. Statistical analysis

Data were presented as mean ± standard for at least three separate determinations for each group. Statistical analysis was performed using SPSS version 25.0 (IBM Corp.). The Student's-t test analysis and one-way ANOVA procedure followed by Tukey test were used to determine whether the difference among groups was statistically significant. Correlations between gut microbiota and differential metabolites were calculated by spearman correlation analysis. *$p < 0.05$, **$p < 0.01$, ***$p < 0.001$, #$p < 0.05$, ##$p < 0.01$, ###$p < 0.001$ were considered to have statistical significance.

3. Results

3.1. TFRD treatment could reduce the effects of OVX-induced OP

In this experiment, the rats were ovariectomized to construct OP model. As shown in Fig. 1A-F, compared with sham 1 group, the number of bone trabeculae decreased and its microstructure was destroyed in model 1 group. In addition, the bone trabecular density of model 1 group was also significantly lower than sham1 group (Figs. 1G). The result of HE staining, BMD analysis and micro-CT analysis indicated that the OVX rat model was successfully established 12 weeks after ovariectomy. As shown in Figs. 2A-G,

the HE staining, BMD and micro-CT analysis showed TFRD and ALN group improved the bone loss and bone ultrastructure in OVX rats after 12-week oral administration of TFRD and ALN treatment compared with model 2 group. The results indicated TFRD treatment could reduce the effects of OVX-induced OP.

3.2. TFRD treatment altered community composition and abundance of gut microbiota in OVX-induced osteoporosis

The principal coordinates analysis (PCoA) showed that there was difference in the microbial community composition of the model group compared with the sham group, while the change in the TFRD group was more significant compared with the model group (Fig. 3A). In order to analyze the specific changes of gut microbiota, the relative abundance analysis was conducted (top 20). At species level, the relative abundance of *Akkermansia_muciniphila* in TFRD group significantly increased compared with the model group (Fig. 3B). As shown in Fig. 3C, the Veen diagram showed the number of species in the three groups, including 322 common species. Based on criteria of |Log2(Fold_change_value)| > 1 and adjusted P value < 0.05, the differential microbiota was screened at species level, and cluster analysis of which shown in heatmap (Fig. 3D, top 50 relative abundance). Combined with the screening results and heat map, it was found that the relative abundance of 17 differential microbiota with OVX interventions was reversed after TFRD treatment, including *Phascolarctobacterium_succinatutens, Lachnospiraceae_bacterium_ GAM79, Acidaminococcus_intestini, Bacteroides_pyogenes, Akkermansia_muciniphila, Corynebacterium_stationis, Faecalibacterium_sp.AF28-13AC, Jeotgalicoccus_halotolerans, Bacteroides_coprophilus, Mediterranea_massiliensis, and Prevotella_sp. P4-98, P4-67, P4-119, AM42-24*, shown in Table 1. The LDA Effect Size (LEfSe) analysis was used to search for the stable differential microbiota between groups. The results of LEfSe showed the relative abundance of *g__Phascolarctobacterium* and *s__Phascolarctobacterium_succinatutens* in model group was significantly higher than sham group and TFRD group (Fig. 3E). The results of metagenomics indicated TFRD treatment could alter community composition and abundance of gut microbiota in OVX-induced OP.

Table 1
At the species level, the changes of relative abundance of 17 differential microbiota in sham, model and TFRD group.

Name	sham_vs_model_de	sham_vs_model_logfc	model_vs_TFRD_de	model_vs_TFRD_logfc
Prevotella_sp.P4-98	up	6.982	down	-7.588
Prevotella_sp.AM42-24	up	6.959	down	-7.153
Phascolarctobacterium_succinatutens	up	6.72	down	-6.926
Lachnospiraceae_bacterium_GAM79	up	4.293	down	-6.647
Prevotella_sp.P4-67	up	6.215	down	-6.336
Acidaminococcus_intestini	up	6.277	down	-6.245
Corynebacterium_stationis	up	6.07	down	-5.917
Prevotella_sp.P5-60	up	5.005	down	-5.083
Prevotella_bryantii	up	4.753	down	-5.042
Faecalibacterium_sp.AF28-13AC	up	5.107	down	-4.995
Ruminococcus_sp.AM28-13	up	3.3	down	-4.838
Jeotgalicoccus_halotolerans	up	4.789	down	-4.542

Name	sham_vs_model_de	sham_vs_model_logfc	model_vs_TFRD_de	model_vs_TFRD_logfc
Bacteroides_coprophilus	up	4.793	down	-4.366
Mediterranea_massiliensis	up	4.126	down	-3.841
Prevotella_sp.P4-119	up	2.564	down	-2.941
Bacteroides_pyogenes	up	3.113	down	-2.768
Akkermansia_muciniphila	down	-1.752	up	4.741

3.3. TFRD treatment regulate metabolites and related pathways in OVX-induced osteoporosis

The untargeted metabolomics about serum of rats was carried out by LC-MS to study the metabolic character of TFRD. As shown in Fig. 4A, the principal components analysis (PCA) showed the samples among group showed significant difference in the positive and negative mode. Based on criteria of VIP > 1 and $p < 0.05$, 216 the differential metabolites were screened, and cluster analysis of which showed in Fig. 4B, C. The 8 differential metabolites pathway was found by metabolic pathway analysis including Protein digestion and absorption, Central carbon metabolism in cancer, Phenylalanine metabolism, Aminoacyl-tRNA biosynthesis, Mineral absorption, Arginine biosynthesis, Phenylalanine, tyrosine and tryptophan biosynthesis and ABC transporters, shown in Fig. 3D. As shown in Fig. 5 and Table 2, considering the small sample size, other 11 metabolites with reverse trend including Succinic acid, Histamine, Salicylic acid, Biotin, Deoxyuridine, Neocnidilide, Tubocurarine, Azelaic acid, Ecdysone, L-Phenylalanine and 3,4-Dihydroxymandelic acid were also selected as differential metabolites except for Gamma-terpinene, Maleamate and L-Malic acid. The results of untargeted metabolomics indicated TFRD treatment could regulate metabolites and related pathways in OVX-induced OP.

Table 2
The changes of 14 differential metabolites in sham, model and TFRD group.

Name	VIP	p.value	Tukeys HSD
Gamma-terpinene	1.392570825	2.50E-09	MODEL-SHAM; TFRD-MODEL
Biotin	1.244967001	0.00437288	MODEL-SHAM;
Maleamate	1.186820731	1.61E-06	MODEL-SHAM; TFRD-MODEL
Ecdysone	1.159940656	0.000477135	MODEL-SHAM;
Histamine	1.345676879	9.99E-08	MODEL-SHAM;
Neocnidilide	1.14603809	4.09E-05	MODEL-SHAM;
L-Malic acid	1.272011698	8.14E-06	MODEL-SHAM; TFRD-MODEL
Succinic acid	1.364330632	3.69E-05	MODEL-SHAM;
Tubocurarine	1.148841128	0.000113794	MODEL-SHAM;
Salicylic acid	1.054348091	0.002405445	MODEL-SHAM
3,4-Dihydroxymandelic acid	1.032052275	0.027278675	MODEL-SHAM
L-Phenylalanine	1.410722026	0.006148879	TFRD-MODEL
Azelaic acid	1.03447778	0.028287352	MODEL-SHAM
Deoxyuridine	1.004110563	0.012568633	MODEL-SHAM

3.4. TFRD treatment increased content of SCFAs in OVX-induced osteoporosis

In this experiment, it was found that TFRD treatment had an effect on the gut microbiota and metabolomic changes of OVX rats. Previous studies found that SCFAs, one of the most important metabolites of gut microbiota, effectively regulated osteoclast metabolism and played an important role in the prevention and treatment of metabolic syndrome. In order to study the mechanism of TFRD against OP, the content of SCFAs was detected in feces. As shown in Fig. 6A, compared with sham group, the concentration of acetic acid decreased in the OVX group. There was significant difference between the OVX group and TFRD treatment group in the amount of acetic acid ($p < 0.05$). Therefore, the acetic acid of gut microbiota in rats decreased significantly after ovariectomy, while increased significantly after TFRD treatment, indicating TFRD treatment could increase content of SCFAs in OVX-induced OP.

3.5. Correlation analysis of gut microbiota and related metabolites

In present study, spearman correlation analysis was used to further analyze relationship between gut microbiota and related metabolites. As shown in Fig. 6C, it was found that 17 differential species reversed by TFRD were negatively or positively associated with at least one differential metabolites. 10 differential species were negatively correlated with Succinic acid. In addition, *Akkermansia muciniphila* were positively correlated with L-Phenylalanine. According to results of the previous metabolic pathway analysis, it was found that L-Phenylalanine and Succinic acid both enriched in Phenylalanine metabolism, a key pathway for TFRD to regulate bone metabolism. In conclusion, gut microbiota such as *Akkermansia muciniphila* might be closely related to phenylalanine metabolism.

4. Discussion

In this study, the efficacy and mechanism of TFRD on OVX-induced OP was explored. HE staining, micro-CT and BMD analysis were used to observe pharmacological effects of TFRD against OVX-induced OP, and the results of which indicated TFRD could improve the bone loss and bone ultrastructure in OVX rats. Subsequently, multiple omics analysis including metagenomic, untargeted and SCFAs metabolomics were used to uncover the mechanism of TFRD against OP. The multiomics analysis revealed that TFRD regulated changes of gut microbiota, metabolites and SCFAs in OVX-induced OP. Furthermore, according to results of untargeted metabolomics analysis, it was found several metabolic pathways such as phenylalanine metabolism, phenylalanine, tyrosine and tryptophan biosynthesis and so on might play an important role in TFRD against OP. At last, spearman correlation analysis showed that gut microbiota such as *Akkermansia muciniphila* might be closely related to phenylalanine metabolism.

The OVX model, a classical PMOP model, was selected in this experiment[23]. As expected, BMD of rats significantly decrease after ovariectomy. In addition, the results of HE staining showed the bone trabeculae of rats were thinner the bone and sparser arrangement in model group compared with sham group, indicating OVX-induced OP model was successfully established. After 12-week TFRD treatment, the reduction of bone mass was significantly improved. Nowadays, microstructural determinants are necessary in assessing the true impact of treatment on trabecular bone quality[24]. Therefore, besides HE staining and BMD analysis, micro-CT analysis has also been used in pharmacodynamic evaluation of TFRD against OP. The results of the micro-CT showed that the morphometric parameters (BV/TV and Tb.N) of the trabecular bone at the distal femur were improved in the OVX rats in response to 12-week TFRD treatment. Furthermore, the TFRD treatment decreased the OVX-induced changes of the Tb.Sp and SMI, indicating that the deterioration of trabecular bone microstructure was significantly improved. Previous studies showed that TFRD could increase number and density of bone trabeculae, and improve the morphology of bone tissue and the biomechanical strength of osteoporotic rats, which is consistent with our above experimental results[25].

The gut microbiota has been verified to be closely associated with OP[26]. In this study, gut microbiota in the feces of rats was analyzed by metagenomics to identify relationship between TFRD against OP and gut microbiota. PCoA results showed that the microbial community in OVX group was different from that in sham group. The gut microbiota composition changed after TFRD treatment. In addition, studies have

confirmed that flavonoids can regulate the composition of human gut microbiota[27]. Therefore, PCoA results indicated that ovariectomy caused gut microbiota disorder, and TFRD could affect bone metabolism by altering the composition and distribution of gut microbiota. At species level, after TFRD treatment the abundance of *Phascolarctobacterium_succinatutens, Lachnospiraceae_bacterium_GAM79, Acidaminococcus_intestini, Bacteroides_pyogenes, Corynebacterium_stationis, Faecalibacterium_sp.AF28-13AC, Jeotgalicoccus_halotolerans, Bacteroides_coprophilus, Mediterranea_massiliensis, and Prevotella_sp. P4-98, P4-67, P4-119, AM42-24* were decreased, while *Akkermansia_muciniphila* was significantly increased. Several studies have found gut microbiota at genus level such as *Phascolarctobacterium, Faecalibacterium, Bacteroides* and *Prevotella* were increased in the osteoporotic animals and people by 16S rRNA sequencing[28,29,30]. *Bacteroides_pyogenes* and *Bacteroides_coprophilus* belong to *Bacteroides* which is considered to associate with reduced BMD and T-score at lumbar spines[31]. *Akkermansia muciniphila*, a symbiotic bacterium of the mucus layer, is considered to be a promising probiotic and play a role in preventing bone metabolic disorders because of its properties of anti-inflammatory and reducing bone destruction[32,33,34]. Studies have reported that colonization with gut microbiota from children could reverse OVX induced bone metabolic imbalance and OP by increasing *Akkermansia muciniphila*, indicating that *Akkermansia muciniphila* has an effect against OP[8]. Therefore, TFRD could reduce the effects of OVX-induced OP by altering community composition and abundance of gut microbiota.

It was found that alterations of gut microbiota and metabolites in feces and serum were responsible for the occurrence and development of OP[35]. In this study, untargeted metabolomics analysis in serum was carried out to explore the effect of TFRD on metabolism of OVX-induced OP. PCA results showed that there were significant differences in metabolites between the sham group and model group. The serum metabolites under the action of TFRD showed a trend towards the sham group. In addition, our study found 14 differential metabolites including Gamma-terpinene, L-Malic acid, Succinic acid, Maleamate, Histamine, Salicylic acid, Biotin, Deoxyuridine, Neocnidilide, Tubocurarine, Azelaic acid, Ecdysone, L-Phenylalanine, 3,4-Dihydroxymandelic acid under the action of TFRD. The co-polymers formed by recombinant osteoprotegerin and Maleamate can further improve the therapeutic effect of OP and show stronger bone resorption inhibitory activity[36]. It is reported that the uptake disorder of key molecules such as biotin caused by SLC5A6 gene mutation can seriously affect the development of bone, brain and immunity. This kind of population can be improved after biotin supplementation[37]. Osteopontin, a bone matrix protein involved in the regulation of absorption, can be inhibited by D-tubocurarine, and then inhibit OP induced by nicotine[38]. β-Ecdysone has a protective effect on bone and can promote the osteogenic differentiation of bone marrow mesenchymal stem cells[39]. Furthermore, the results of metabolic pathway analysis revealed several metabolic pathways such as phenylalanine metabolism, phenylalanine, tyrosine and tryptophan biosynthesis and so on might play an important role in TFRD against OP. It is reported that *Drynaria roosii* Nakaike may prevent OP by interfering with phenylalanine metabolism and tryptophan metabolism in rats, which also indirectly confirms our experimental results[40]. L-phenylalanine, one of the essential aromatic amino acids with physiological activity, can increase

protein synthesis rates of bone tissue[41]. In addition, tyrosine, produced by the catalysis of phenylalanine, phosphorylation of which affects the interaction of Cbl-PI3K. The elimination of this effect will disturb bone homeostasis and affect osteoclast function and osteoblast proliferation[42].

Spearman correlation analysis showed that most of differential metabolites were positively or negatively correlated with gut microbial species, indicating that TFRD against OP might be closely related to the changes of gut microbiota and related metabolites. Interestingly, L-phenylalanine and succinic acid from phenylalanine metabolism are significantly correlated with *Akkermansia muciniphila*, *Phascolarctobacterium succinatutens* and other gut microbiota, which is also the focus of our study. Several studies have found *Akkermansia muciniphila* could attenuate colonic inflammation by regulating tryptophan metabolism[43]. Phenylalanine and tryptophan are essential aromatic amino acid for human body. Therefore, it was speculated that *Akkermansia muciniphila* and phenylalanine metabolism might play crucial roles in TFRD against OP.

In recent years, SCFA released by gut microbiota has become a hot spot in the research of OP because it plays an important role in regulation of osteoclast metabolism and bone homeostasis[44]. Therefore, besides untargeted metabolomics in serum, SCFAs metabolomics analysis in feces was also carried out in this experiment. In this study, acetic acid of SCFAs in feces decreased significantly after ovariectomy, and TFRD reversed this change. It has been reported that the content of SCFA including acetic acid and butyric acid in feces of OVX-induced rats decreased, which also confirmed our results[45]. Studies have confirmed that flavonoids can stimulate gut microbiota to produce SCFAs, especially acetic acid and butyric acid[46]. Furthermore, according to a new study, *Akkermansia muciniphila* could promote secretion of SCFA including acetic acid, butyric acid and so on[47]. Therefore, TFRD might reduce the effects of OVX-induced OP by increasing SCFA such as acetic acid.

There are some limitations to the current study that need to be considered. In this research, only integrated metagenomic and metabolomic analyses were carried out, the detailed mechanisms of gut microbiota need to be further explored. We plan to transplant fecal samples from TFRD rats into OVX-induced OP rats and observe the changes of plasma, composition and function of intestinal flora among transplanted rats, TFRD group, normal group and model group and oral administration of *AKK* bacteria to detect changes in metabolites.

5. Conclusion

Based on pharmacodynamics, it was found TFRD treatment could reduce the effects of OVX-induced OP. The metagenomics analysis indicated TFRD treatment could alter community composition and abundance of gut microbiota in OVX-induced OP. Of those, the abundance of *Akkermansia muciniphila* significantly increased. The metabolomics analysis showed several metabolites changed, and acetic acid in SCFA increased after TFRD treatment. Spearman correlation analysis indicated gut microbiota such as *Akkermansia muciniphila* might be closely related to several metabolites and metabolic pathways. In this study, it was speculated that gut microbiota especially *Akkermansia muciniphila* and related metabolites

might play an important role in TFRD against OP. This conclusion provides a new way to further clarify the molecular mechanism of TFRD against OP, but it still needs to be further verified to obtain direct evidence that TFRD regulates gut microbiota to treat OP.

Abbreviations

TFRD	Total flavonoids of Rhizoma Drynariae
OP	osteoporosis
H&E	hematoxylin-eosin
micro-CT	micro computed tomography
BMD	bone mineral density
OVX	ovariectomized
SCFAs	short chain fatty acids
PMOP	postmenopausal osteoporosis
LPS	lipopolysaccharide
TCM	traditional Chinese medicine
RANKL	receptor activator of nuclear factor kappa-B ligand
ALN	alendronate
UHPLC-ESI-Q-TOF-MS	ultra-high-performance liquid chromatography coupled with electrospray ionization quadrupole time-of-flight mass spectrometry
EDTA	ethylenediaminetetraacetic acid
LC-MS	Liquid Chromatography-Mass Spectrometry
PcoA	principal coordinates analysis
LefSe	LDA Effect Size

Declarations

Data availability statement

The datasets presented in this study can be found in online repositories. The names of the repository/repositories and accession number(s) can be found below: NCBI, SRA, PRJNA816829. https: //www.ncbi.nlm.nih.gov /bioproject/PRJNA816829.

Conflicts of interest

The authors have declared no conflicts of interest.

References

1. Zhou, Y. *et al*. Cytokine-scavenging nanodecoys reconstruct osteoclast/osteoblast balance toward the treatment of postmenopausal osteoporosis. Sci Adv 7(48), eabl6432.(2021)
2. Xu, X. *et al.* Intestinal microbiota: a potential target for the treatment of postmenopausal osteoporosis. Bone Res 5, 17046.(2017)
3. Chevalier, C. *et al.* Warmth Prevents Bone Loss Through the Gut Microbiota. Cell Metab 32(4), 575–590.e577.(2020)
4. He, J. *et al*. Gut microbiota and metabolite alterations associated with reduced bone mineral density or bone metabolic indexes in postmenopausal osteoporosis. Aging (Albany NY) 12(9), 8583–8604. (2020)
5. Qin, Q. *et al*. The Relationship Between Osteoporosis and Intestinal Microbes in the Henan Province of China. Front Cell Dev Biol 9, 752990.(2021)
6. Villa, C.R., Ward, W.E., Comelli, E.M. Gut microbiota-bone axis. Crit Rev Food Sci Nutr 57(8), 1664–1672.(2017)
7. Mei, F. *et al.* Arecanut (Areca catechu L.) Seed Polyphenol-Ameliorated Osteoporosis by Altering Gut Microbiome via LYZ and the Immune System in Estrogen-Deficient Rats. J Agric Food Chem 69(1), 246–258.(2021)
8. Liu, J.H. *et al.* Extracellular Vesicles from Child Gut Microbiota Enter into Bone to Preserve Bone Mass and Strength. Adv Sci (Weinh) 8(9), 2004831.(2021)
9. Hao, M.L. *et al.* Gut microbiota: an overlooked factor that plays a significant role in osteoporosis. J Int Med Res 47(9), 4095–4103.(2019)
10. Lin, J. *et al.* Chinese single herbs and active ingredients for postmenopausal osteoporosis: From preclinical evidence to action mechanism. Biosci Trends 11(5), 496–506.(2017)
11. Zhang, N.D. *et al*. Traditional Chinese medicine formulas for the treatment of osteoporosis: Implication for antiosteoporotic drug discovery. J Ethnopharmacol 189, 61–80.(2016)
12. Zhang, Y. *et al*. Tissue Distribution of Total Flavonoids Extracts of Drynariae Rhizoma in Young and Old Rats by UPLC-MS/MS Determination. J Anal Methods Chem 2022, 2447945.(2022)
13. Sun, W. *et al*. Total flavonoids of rhizoma drynariae ameliorates bone formation and mineralization in BMP-Smad signaling pathway induced large tibial defect rats. Biomed Pharmacother 138, 111480. (2021)
14. Zhao, K. *et al.* Rhizoma drynariae total flavonoids inhibit the inflammatory response and matrix degeneration via MAPK pathway in a rat degenerative cervical intervertebral disc model. Biomed Pharmacother 138, 111466.(2021)

15. Zhang, Y. *et al.* Total flavonoids from Rhizoma Drynariae (Gusuibu) for treating osteoporotic fractures: implication in clinical practice. Drug Des Devel Ther 11, 1881–1890.(2017)
16. Shen, Z. *et al.* Total Flavonoids of Rhizoma Drynariae Enhances Angiogenic-Osteogenic Coupling During Distraction Osteogenesis by Promoting Type H Vessel Formation Through PDGF-BB/PDGFR-β Instead of HIF-1α/ VEGF Axis. Front Pharmacol 11, 503524.(2020)
17. Song, S.H. *et al*. Effects of total flavonoids from Drynariae Rhizoma prevent bone loss in vivo and in vitro. Bone Rep 5, 262–273.(2016)
18. Murota, K., Nakamura, Y., Uehara, M. Flavonoid metabolism: the interaction of metabolites and gut microbiota. Biosci Biotechnol Biochem 82(4), 600–610.(2018)
19. Yu, H., Zheng, R., Su, W., Xing, J., Wang, Y. Metabolism characteristics and pharmacological insights of flavonoids based on the intestinal bacteria. Acta Pharmaceutica Sinica 56(7),1757–1768 + 1748. (2021)
20. Stephens, M. *et al.* Murine femur micro-computed tomography and biomechanical datasets for an ovariectomy-induced osteoporosis model. Sci Data 8(1), 240.(2021)
21. Vakili, S., Zal, F., Mostafavi-Pour, Z., Savardashtaki, A., Koohpeyma, F. Quercetin and vitamin E alleviate ovariectomy-induced osteoporosis by modulating autophagy and apoptosis in rat bone cells. J Cell Physiol 236(5), 3495–3509.(2021)
22. Zhang, F. *et al*. Total Flavonoids of Drynariae Rhizoma Improve Glucocorticoid-Induced Osteoporosis of Rats: UHPLC-MS-Based Qualitative Analysis, Network Pharmacology Strategy and Pharmacodynamic Validation. Front Endocrinol (Lausanne) 13, 920931.(2022)
23. Mathavan, N., Turunen, M.J., Tägil, M., Isaksson, H. Characterising bone material composition and structure in the ovariectomized (OVX) rat model of osteoporosis. Calcif Tissue Int 97(2), 134–144. (2015)
24. Marinozzi, F. *et al*. Technique for bone volume measurement from human femur head samples by classification of micro-CT image histograms. Ann Ist Super Sanita 49(3), 300–305.(2013)
25. Mu, P., Hu, Y., Ma, X., Shi, J., Zhong, Z., Huang, L. Total flavonoids of Rhizoma Drynariae combined with calcium attenuate osteoporosis by reducing reactive oxygen species generation. Exp Ther Med 21(6), 618.(2021)
26. Wang, J. *et al.* Diversity analysis of gut microbiota in osteoporosis and osteopenia patients. PeerJ 5, e3450.(2017)
27. Hidalgo, M. *et al*. Metabolism of anthocyanins by human gut microflora and their influence on gut bacterial growth. J Agric Food Chem 60(15), 3882–3890.(2012)
28. Ling, C.W. *et al.* The Association of Gut Microbiota With Osteoporosis Is Mediated by Amino Acid Metabolism: Multiomics in a Large Cohort. J Clin Endocrinol Metab 106(10), e3852-e386(2021)
29. Wang, N., Meng, F., Ma, S., Fu, L. Species-level gut microbiota analysis in ovariectomized osteoporotic rats by Shallow shotgun sequencing. Gene 817, 146205.(2022)

30. Xu, Z. *et al.* Gut Microbiome Reveals Specific Dysbiosis in Primary Osteoporosis. Front Cell Infect Microbiol 10, 160.(2020)
31. Wei, M. *et al.* High-Throughput Absolute Quantification Sequencing Revealed Osteoporosis-Related Gut Microbiota Alterations in Han Chinese Elderly. Front Cell Infect Microbiol 11, 630372.(2021)
32. Huck, O. *et al.* Akkermansia muciniphila reduces Porphyromonas gingivalis-induced inflammation and periodontal bone destruction. J Clin Periodontol 47(2), 202–212.(2020)
33. Keshavarz Azizi Raftar, S. *et al.* Assessment of fecal Akkermansia muciniphila in patients with osteoporosis and osteopenia: a pilot study. J Diabetes Metab Disord 20(1), 279–284.(2021)
34. Zhang, T., Li, Q., Cheng, L., Buch, H., Zhang, F. Akkermansia muciniphila is a promising probiotic. Microb Biotechnol 12(6), 1109–1125.(2019)
35. Wen, K. *et al.* Fecal and Serum Metabolomic Signatures and Microbial Community Profiling of Postmenopausal Osteoporosis Mice Model. Front Cell Infect Microbiol 10, 535310.(2020)
36. Miyaji, Y. *et al.* Novel comb-shaped PEG modification enhances the osteoclastic inhibitory effect and bone delivery of osteoprotegerin after intravenous administration in ovariectomized rats. Pharm Res 29(11), 3143–3155.(2012)
37. Subramanian, V.S., Constantinescu, A.R., Benke, P.J., Said, H.M. Mutations in SLC5A6 associated with brain, immune, bone, and intestinal dysfunction in a young child. Hum Genet 136(2), 253–261. (2017)
38. Walker, L.M., Preston, M.R., Magnay, J.L., Thomas, P.B., El Haj, A.J. Nicotinic regulation of c-fos and osteopontin expression in human-derived osteoblast-like cells and human trabecular bone organ culture. Bone 28(6), 603–608.(2001)
39. You, W.L., Xu, Z.L. β-ecdysone promotes osteogenic differentiation of bone marrow mesenchymal stem cells. J Gene Med 22(9), e3207.(2020)
40. Liu, X., Zhang, S., Lu, X., Zheng, S., Li, F., Xiong, Z. Metabonomic study on the anti-osteoporosis effect of Rhizoma Drynariae and its action mechanism using ultra-performance liquid chromatography-tandem mass spectrometry. J Ethnopharmacol 139(1), 311–317.(2012)
41. Smeets, J.S.J. *et al.* Protein synthesis rates of muscle, tendon, ligament, cartilage, and bone tissue in vivo in humans. PLoS One 14(11), e0224745.(2019)
42. Brennan, T., Adapala, N.S., Barbe, M.F., Yingling, V., Sanjay, A. Abrogation of Cbl-PI3K interaction increases bone formation and osteoblast proliferation. Calcif Tissue Int 89(5), 396–410.(2011)
43. Mao, S., Zhu, W. Effects of six flavonoid compounds addition on short-chain fatty acids production and human fecal microbial community change during in vitro fermentation. African Journal of Microbiology Research 5(26), 4484–4491.(2011)
44. Gu, Z. *et al.* Akkermansia muciniphila and its outer protein Amuc_1100 regulates tryptophan metabolism in colitis. Food Funct 12(20), 10184–10195.(2021)
45. Li, B. *et al.* Puerarin improves the bone micro-environment to inhibit OVX-induced osteoporosis via modulating SCFAs released by the gut microbiota and repairing intestinal mucosal integrity. Biomed

Pharmacother 132, 110923.(2020)

46. Lucas, S. *et al.* Short-chain fatty acids regulate systemic bone mass and protect from pathological bone loss. Nat Commun 9(1), 55.(2018)
47. Xia, J. *et al.* Akkermansia muciniphila Ameliorates Acetaminophen-Induced Liver Injury by Regulating Gut Microbial Composition and Metabolism. Microbiol Spectr 10(1), e0159621.(2022)

Figures

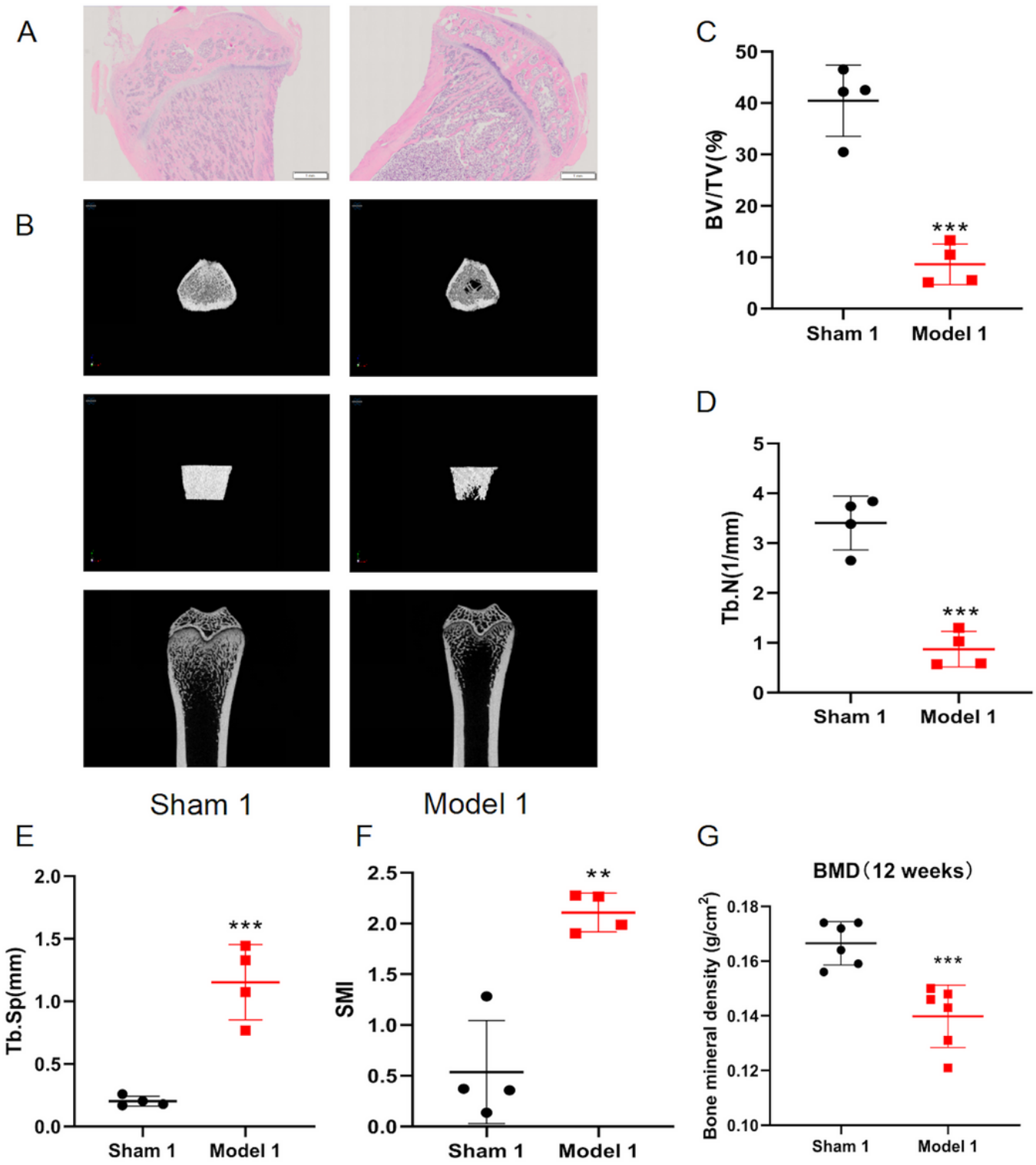

Figure 1

The OVX rat model was successfully established 12 weeks after ovariectomy. **A.**H&E staining about tibial of rats (n=3). **B-H.** Micro-CT analysis about tibial of rats (n=4). **I.** BMD analysis about femur of rats (n=6). Data were expressed as mean±SD, vs. model group, *$p < 0.05$, **$p < 0.01$, ***$p < 0.001$.

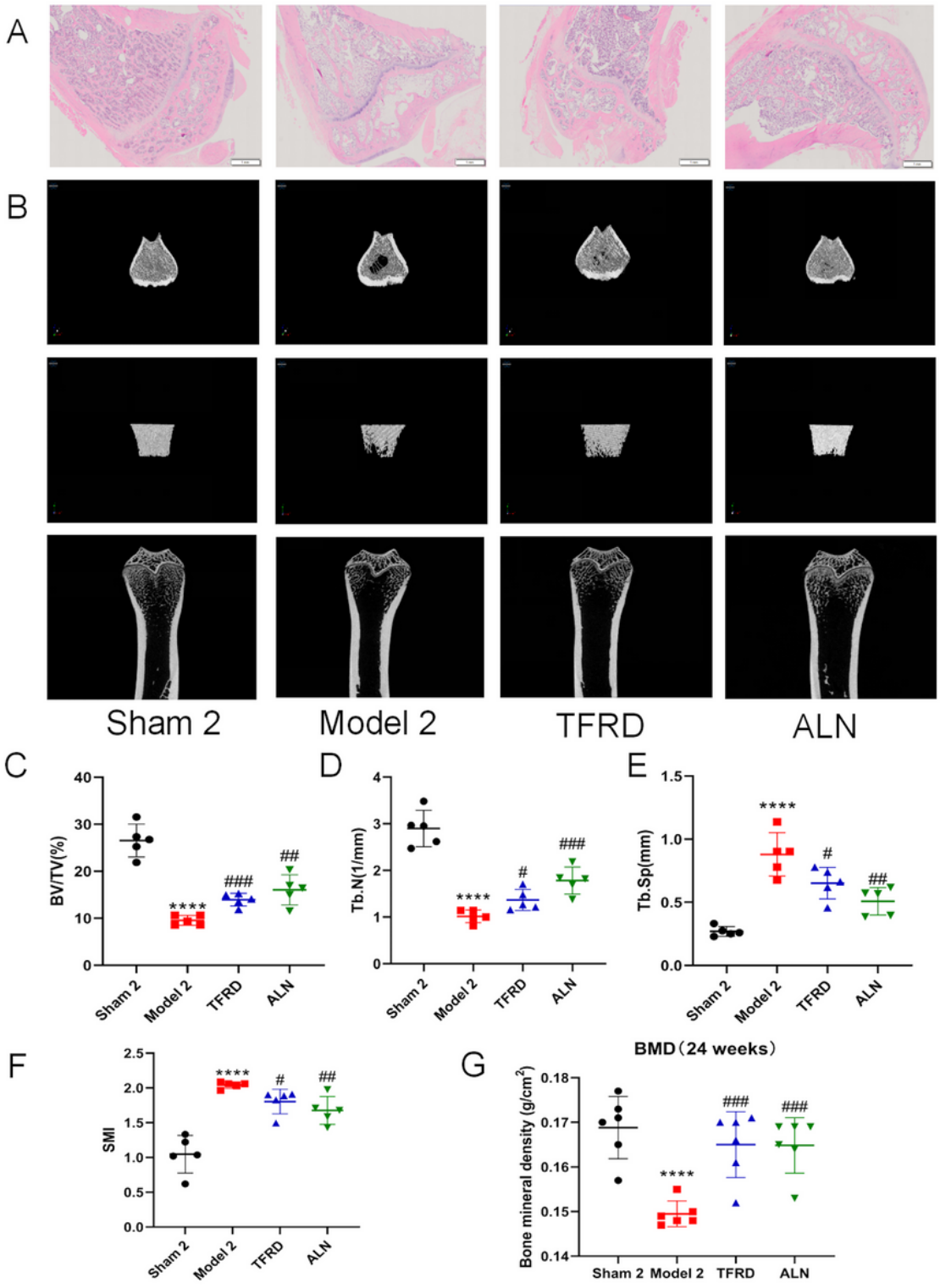

Figure 2

TFRD treatment improve OVX-induced OP. After the establishment of OVX rat model (12 weeks), rats were orally administrated TFRD (67.5 mg/kg), ALN (1 mg/kg) or distilled water once a day for 12 weeks. **A.** H&E staining about tibial of rats (n=3). **B-H.** Micro-CT analysis about tibial of rats (n=5). **I.** BMD analysis about femur of rats (n=6). Data were expressed as mean±SD, vs. model group, *$p < 0.05$, **$p < 0.01$, ***$p < 0.001$, vs. the TFRD or ALN group, #$p < 0.05$, ##$p < 0.01$, ###$p < 0.001$.

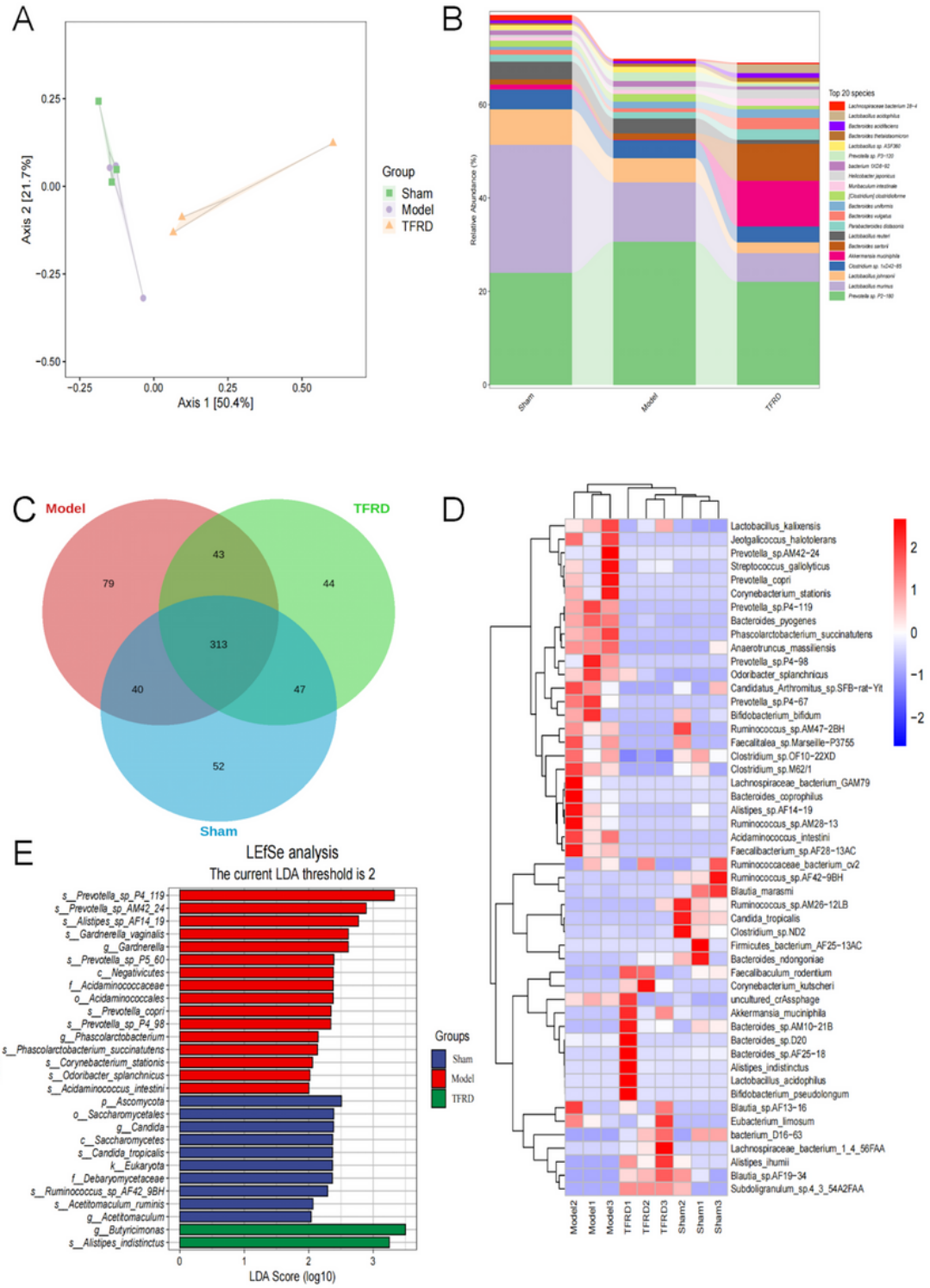

Figure 3

Metagenomics analysis data (n=3). **A.** PCoA about sham, model and TFRD groups. **B.** At the species level, the relative abundances of gut microbiota in sham, model and TFRD groups. **C.** Venn plots about sham, model and TFRD groups. **D.** Heat plot about differential microbiota (top 50). **E.** LEfSe analysis about gut microbiota in sham, model and TFRD groups.

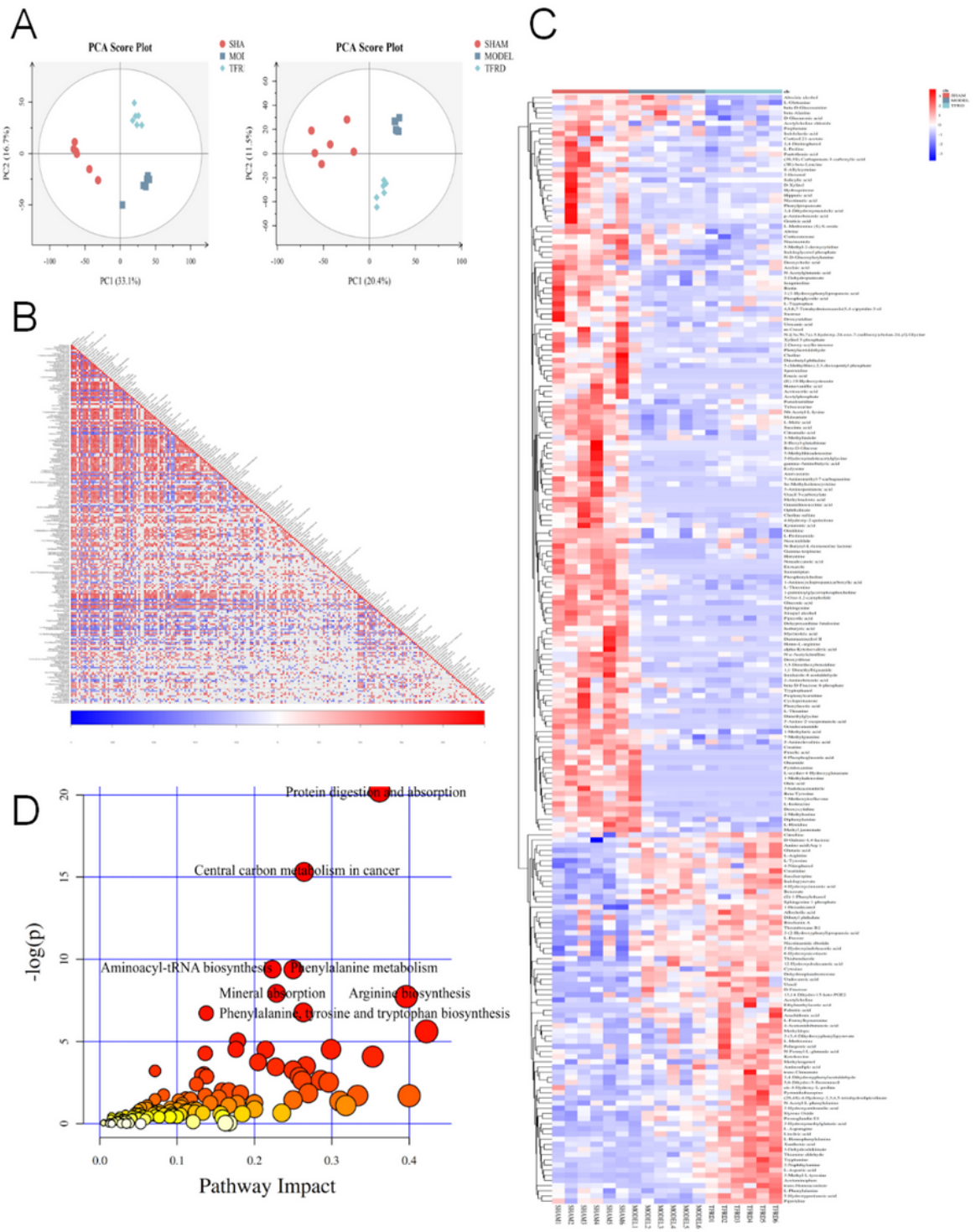

Figure 4

Untargeted metabolomics analysis data (n=6). **A.** PCA about sham, model and TFRD groups. **B.** Heat plot about correlation between differential metabolites. **C.** Heat plot about differential metabolites in sham, model and TFRD groups. **D.** Metabolic pathway about differential metabolites in sham, model and TFRD groups.

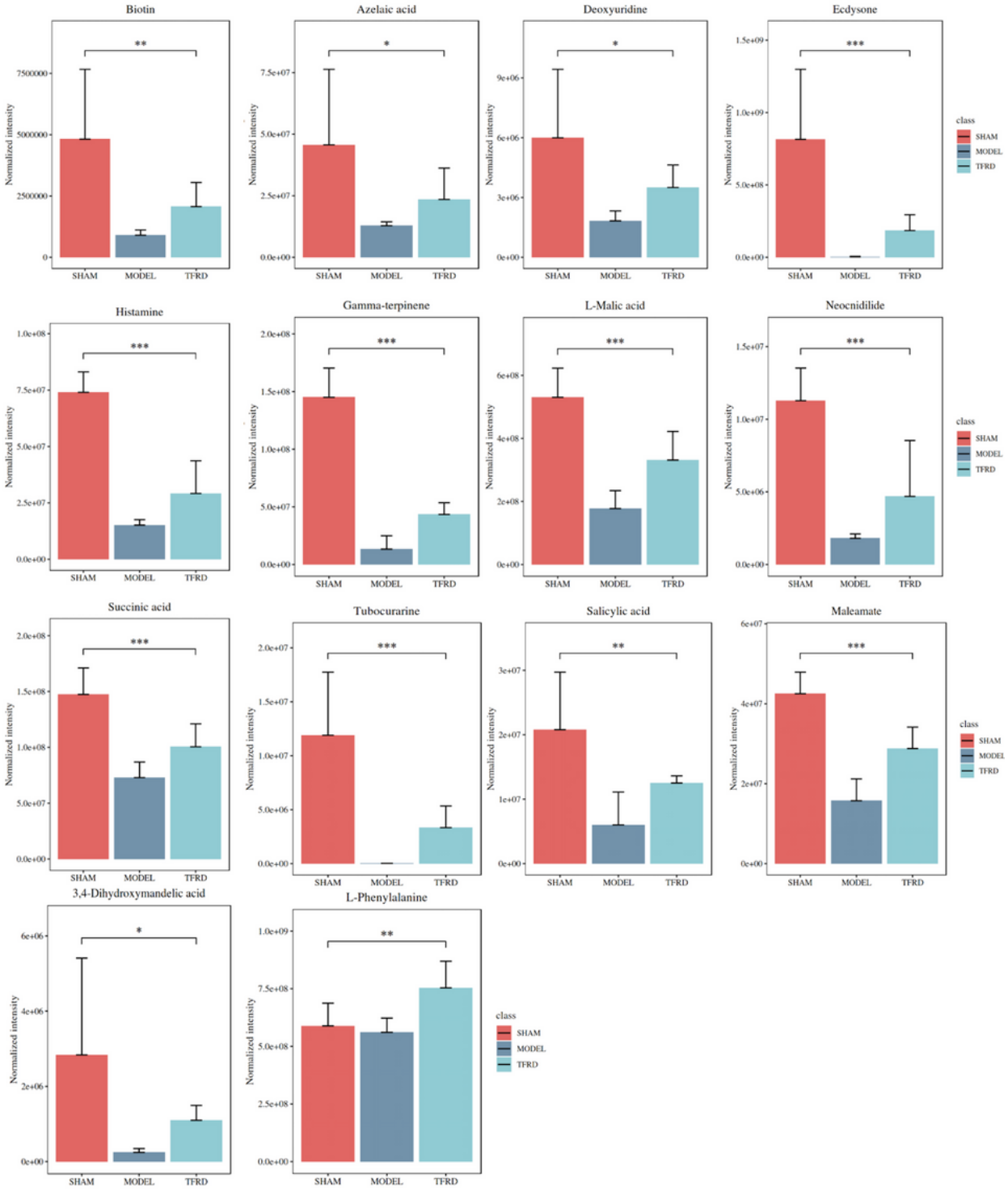

Figure 5

The changes of 14 differential metabolites in sham, model and TFRD group. Data were expressed as mean±SD (n=6), One-way ANOVA procedure followed by Tukey test was used to evaluate the statistical significance, *$p < 0.05$, **$p < 0.01$, ***$p < 0.001$.

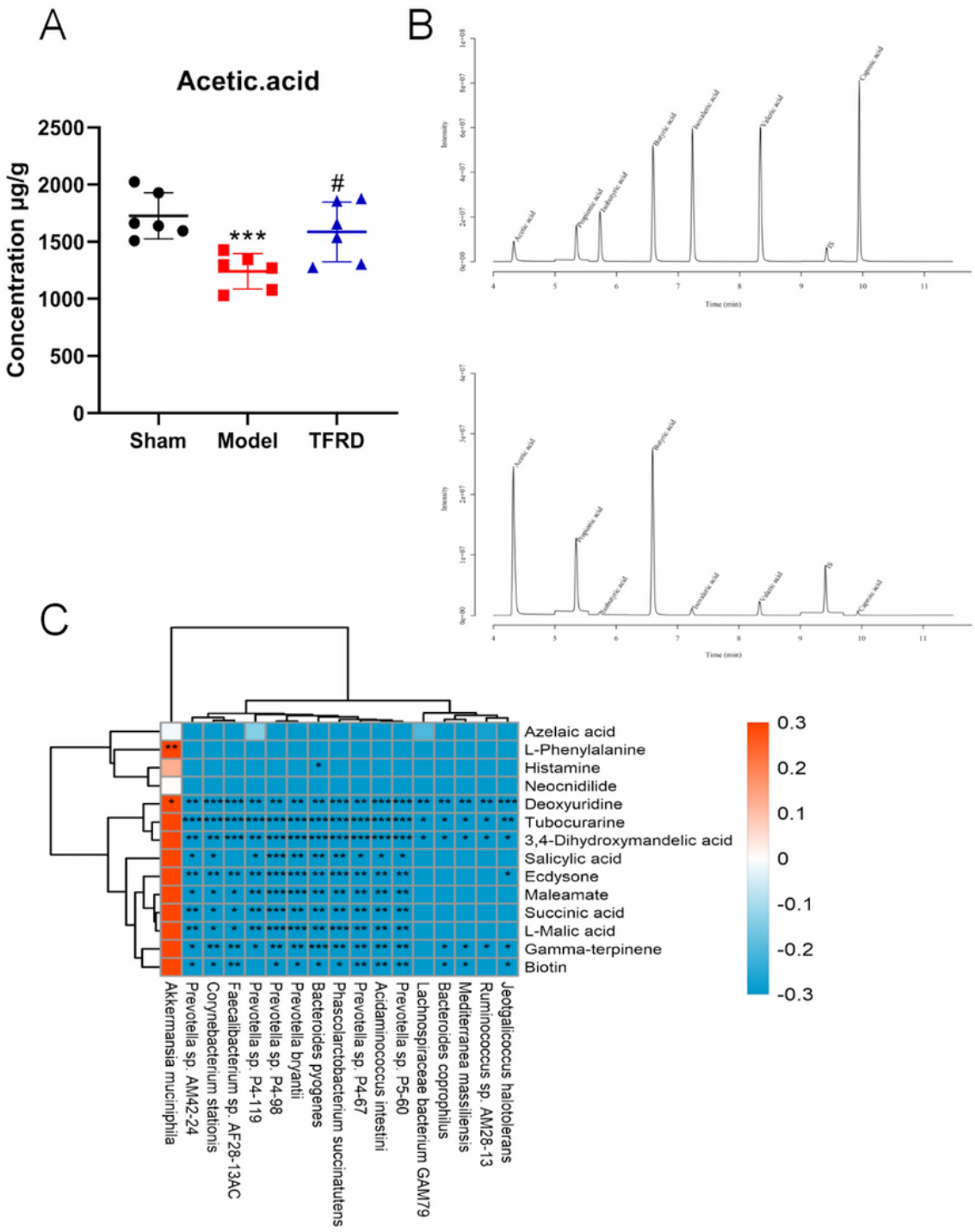

Figure 6

The content of SCFAs in sham, model and TFRD group (n=6). **B.** Sample and mixed TIC diagrams of SCFAs. Data were expressed as mean±SD, vs. model group, *$p < 0.05$, **$p < 0.01$, ***$p < 0.001$, vs. the TFRD or ALN group, #$p < 0.05$, ##$p < 0.01$, ###$p < 0.001$. **C.** Correlation of gut microbiota reversed by TFRD intervention wtih differential metabolites was analyzed by Spearman correlation analysis. Heatmap shows the value of correlation coefficient between gut microbiota and differential metabolites.

*, **, *** indicate the correlation significance ($p < 0.05$, $p < 0.01$ and $p < 0.001$ respectively). Red represents positive correlation and blue represents negative correlation.

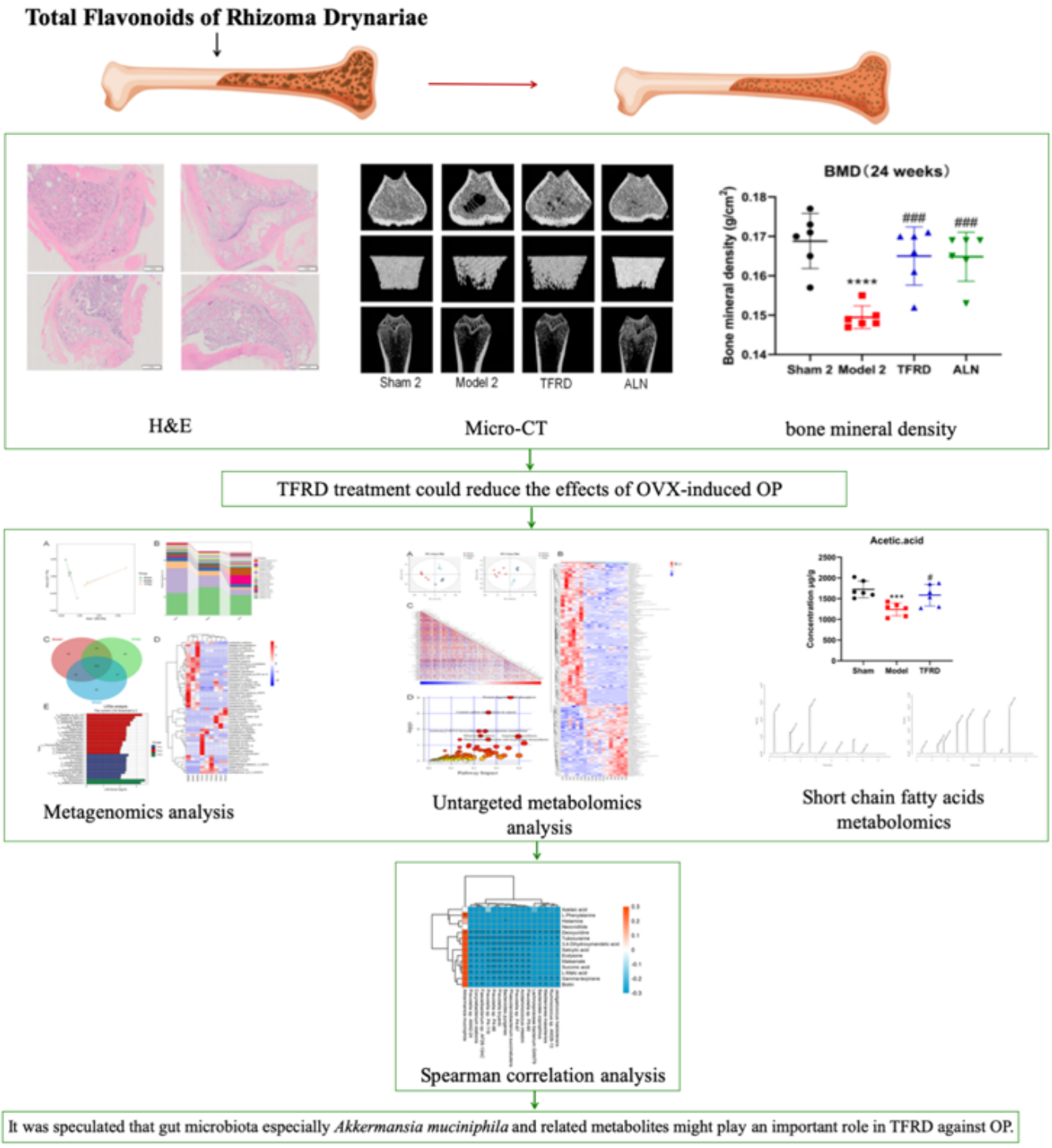

Figure 7

The graphical abstract of this study